University of Zurich[UZH]

Zurich Open Repository and Archive
University of Zurich
University Library
Strickhofstrasse 39
CH-8057 Zurich
www.zora.uzh.ch

Year: 2011

The Evolution of Virulence in RNA Viruses under a Competition–Colonization Trade-Off

Delgado-Eckert, Edgar ; Ojosnegros, Samuel ; Beerenwinkel, Niko

Abstract: RNA viruses exist in large intra-host populations which display great genotypic and phenotypic diversity. We analyze a model of viral competition between two viruses infecting a constantly replenished cell pool. We assume a trade-off between the ability of the virus to colonize new cells (cell killing rate or virulence) and its local competitiveness (replicative success within coinfected cells). We characterize the conditions that allow for viral spread by means of the basic reproductive number and show that a local coexistence equilibrium exists, which is asymptotically stable. At this equilibrium, the less virulent competitor has a reproductive advantage over the more virulent colonizer reflected by a larger equilibrium population size of the competitor. The equilibria at which one virus outcompetes the other one are unstable, i.e., a second virus is always able to permanently invade. We generalize the two-virus model to multiple viral strains, each displaying a different virulence. To account for the large phenotypic diversity in viral populations, we consider a continuous spectrum of virulences and present a continuum limit of this multiple viral strains model that describes the time evolution of an initial continuous distribution of virulence without mutations. We provide a proof of the existence of solutions of the model equations, analytically assess the properties of stationary solutions, and present numerical approximations of solutions for different initial distributions. Our simulations suggest that initial continuous distributions of virulence evolve toward a distribution that is extremely skewed in favor of competitors. At equilibrium, only the least virulent part of the population survives. The discrepancy of this finding in the continuum limit with the two-virus model is attributed to the skewed equilibrium subpopulation sizes and to the transition to a continuum. Consequently, in viral quasispecies with high virulence diversity, the model predicts collective virulence attenuation. This result may contribute to understanding virulence attenuation, which has been reported in several experimental studies.

DOI: https://doi.org/10.1007/s11538-010-9596-2

Posted at the Zurich Open Repository and Archive, University of Zurich
ZORA URL: https://doi.org/10.5167/uzh-81001
Journal Article
Accepted Version

Originally published at:
Delgado-Eckert, Edgar; Ojosnegros, Samuel; Beerenwinkel, Niko (2011). The Evolution of Virulence in RNA Viruses under a Competition–Colonization Trade-Off. Bulletin of Mathematical Biology, 73(8):1881-1908.
DOI: https://doi.org/10.1007/s11538-010-9596-2

The evolution of virulence in RNA viruses under a competition-colonization trade-off

Edgar Delgado-Eckert[1,2,*] Samuel Ojosnegros[1] Niko Beerenwinkel[1,2]

[1]Department of Biosystems Science and Engineering, ETH Zurich, Mattenstrasse 26, 4058 Basel, Switzerland.
[2]Swiss Institute of Bioinformatics.

ABSTRACT

RNA viruses exist in large intra-host populations which display great genotypic and phenotypic diversity. We analyze a model of viral competition between two viruses infecting a constantly replenished cell pool. We assume a trade-off between the ability of the virus to colonize new cells (cell killing rate or virulence) and its local competitiveness (replicative success within coinfected cells). We characterize the conditions that allow for viral spread by means of the basic reproductive number and show that a local coexistence equilibrium exists, which is asymptotically stable. At this equilibrium, the less virulent competitor has a reproductive advantage over the more virulent colonizer. The equilibria at which one virus outcompetes the other one are unstable, i.e., a second virus is always able to permanently invade. One generalization of the model is to consider multiple viral strains, each one displaying a different virulence. However, to account for the large phenotypic diversity in viral populations, we consider a continuous spectrum of virulences and present a continuum limit of this multiple viral strains model that describes the time evolution of an initial continuous distribution of virulence. We provide a proof of the existence of solutions of the model's equations and present numerical approximations of solutions for different initial distributions. Our simulations suggest that initial continuous distributions of virulence evolve towards a stationary distribution that is extremely skewed in favor of competitors. Consequently, collective virulence attenuation takes place. This finding may contribute to understanding the phenomenon of virulence attenuation, which has been reported in previous experimental studies.

Keywords: SIR models of viral infection, Competition-colonization dynamics, RNA virus, Evolution of virulence, Attenuation of virulency.

1. INTRODUCTION

RNA viruses are fast evolving pathogens that can adapt to continuously changing environments. Due to their error-prone replication, large population size, and high turnover, RNA virus populations exist as quasispecies (Eigen et al. (15), Holland et al. (19), Domingo and Holland (14)). The viral mutant spectrum consists of many genetic variants which give rise to diverse phenotypes. This phenotypic diversity is reflected in different traits, including the rate of killing host cells, which is referred to as virulence here.

The concept of virulence has been used in various areas of the life sciences with different meanings. In evolutionary biology, the virulence of a pathogen is defined as the fitness costs to the host that are induced by the pathogen. In epidemiology, the term usually means the pathogen-induced host mortality. In clinical settings, virulence often refers to the severity of disease symptoms induced

*Corresponding author. Email address: edgar.delgado-eckert@mytum.de

by a pathogen. In this article, we consider intra-host virus dynamics and use the term virulence to denote the cell killing rate of a virus infecting tissue. Thus, we apply the epidemiological meaning of virulence to the intra-host viral microepidemics. This definition is related to the macroscopic or inter-host concept of virulence, because, in general, the cell killing rate of a virus affects the course of infection and the mortality of the host.

The evolution of virulence has been studied using experimental and theoretical approaches in a variety of host-pathogen systems and under diverse conditions or assumptions. In the past few decades, the "conventional wisdom" that well-adapted pathogens are avirulent has been replaced by the stricter evolutionary reasoning that successful pathogens exploit their hosts to maximize their number of offspring (Anderson and May (1), Ewald (17)). In fact, basic models of infection biology predict that pathogens will evolve to maximize their basic reproductive number such that the most virulent strain is selected (Bremermann and Thieme (7)).

Because pathogens are exposed to different environmental conditions during their life cycle, they face different types of selective pressure, and adaptation is typically controlled by various phenotypic traits that are not independent. In order to investigate the constraints of adaptability and their impact on the evolution of virulence, several adaptive trade-off theories have been proposed (Bull (8), Frank (18)). These models assume finite resources and make an economic argument by trading off two or more pathogen traits. For example, the trade-off between rapid pathogen reproduction (virulence) and longer transmission time due to longer life time of the host is often considered (Bremermann and Thieme (7), Bonhoeffer et al. (4), Cooper et al. (11)). The virulence-transmission trade-off can give rise to intermediate or increased virulence, but Lenski and May (25) have argued that intermediate virulence levels can lead to reduced virulence in the long run.

Multi-level selection models address the trade-off between pathogen competition within and among hosts. Krakauer and Komarova (23) find intermediate virulence levels when modeling an intracellular trade-off between genome replication capacity and genetic translation applied to polio virus. Coombs et al. (10) integrate the evolutionary and ecological processes of infection and study within- versus between-host competition and find that the strain that maximizes between-host fitness dominates. In the presence of mutation, coexistence is possible and distributions of diverse virulence values with complex dynamics have been observed (Bonhoeffer and Nowak (6), Coombs et al. (10), Boldin and Diekmann (3)). Diverse distributions of virulence are also predicted by a superinfection model without coinfection, but with a hierarchy of competitive dominance among strains (Nowak and May (29), May and Nowak (26)). In this model, the average virulence increases and highly virulent strains can be maintained in the population.

The superinfection model of May and Nowak (26) is closely related to the metapopulation model of Tilman (33), in which coexistence results from spatially structured habitats. A trade-off between the ability of each individual to colonize unoccupied territory and to compete with others for the same habitat patch can result in coexistence of two strategies: competition and colonization. Competitors have an advantage when competing locally for resources, whereas colonizers are more successful in reaching new resources.

Competition-colonization dynamics have recently been demonstrated in an RNA virus *in vitro* using an experimental and theoretical approach (Ojosnegros et al. (31)). In this system, highly virulent viral strains play the role of colonizers, because they kill cells faster and thus replicate faster, which allows faster spread and colonization of new cells. Local competition arises when two or more different viruses infect the same cell and compete for intracellular resources. Competitors manage

to produce more offspring in a cell coinfected together with a colonizer and, at the same time, extend the cell killing time characteristic of a colonizer, a phenomenon known as viral interference.

The competition-colonization coevolutionary dynamics of two different viral strains in cell culture have been described in Ojosnegros et al. (31) by a modification of the basic model of virus dynamics (Nowak and May (28), Perelson and Nelson (32)). The model predicts that the outcome of viral competition for the cell monolayer depends on the initial overall number of viruses per cell. Under low initial density, colonizers produce more total offspring, whereas under high-density conditions, coinfection is more likely to occur and hence competitors have a selective advantage. This prediction was confirmed experimentally.

In the present article, we make a first step towards transferring the results obtained *in vitro* to the *in vivo* situation under the assumption of a competition-colonization trade-off. We extend the basic model of competition-colonization dynamics of two different viral strains in cell culture by replacing the finite cell monolayer with a constantly replenished pool of uninfected cells. Furthermore, to account for the postulated competition-colonization trade-off, we model the intracellular fitness of the viruses during coinfection as being inversely proportional to their respective virulence. Like any adaptive trade-off theory, our model is a metaphor for host-pathogen systems that highlights a specific aspect of the evolution of virulence, namely the interplay between competition and colonization strategies (Frank (18)).

We present a rigorous analytical study of this model and demonstrate that it allows for local asymptotically stable coexistence of competitors and colonizers. Moreover, the less virulent competitor is shown to have a reproductive advantage reflected by its higher abundance and a higher number of cells infected with it at equilibrium.

We generalize this model by considering more than two viral variants. We assume that different viral strains can only be distinguished through their virulences and ask how a distribution of virulences is modified in the course of the infection by the competition-colonization dynamics. In other words, we study the time evolution of a discrete distribution of virulences. While simulation results for a finite number of viral strains will be presented elsewhere (Ojosnegros et al., in preparation), here we account for the very high phenotypic diversity of RNA virus populations by considering the continuum limit of this multiple viral strains model. In the continuum limit, we consider a continuous interval of virulence values and model the time evolution of a continuous distribution of virulence. We provide a proof of the existence of solutions of this model and present numerical approximations.

Our simulations suggest that initial continuous distributions of virulence evolve towards a stationary distribution which is heavily skewed in favor of competitors. Thus, the competition-colonization model predicts attenuation of the virus population. This result might explain previous observations of suppression of high-fitness mutants in various viral systems (de la Torre and Holland (34), Novella et al. (27), Turner and Chao (35), Bull et al. (9)).

This article is organized as follows. In Section 2 we formulate the basic model of two competing viral strains and illustrate our model assumptions. In the Results Section a detailed analytical study of its equilibrium behavior is presented. In Subsection 3.5, the multiple-viral-strains model is introduced and in Subsection 3.6, we derive its continuum limit. The continuous-virulence model is analyzed both analytically and numerically. We close in Section 4 with discussing some of the model assumptions and consequences for the evolution of virulence.

2. FORMULATION OF THE TWO-VIRAL-STRAINS MODEL

Our modeling approach is based on the basic SIR model of virus dynamics (Nowak and May (30),Perelson and Nelson (32)), which we extend in order to model two different viral populations infecting constantly replenished tissue. We model singly infected and superinfected (doubly infected or coinfected) cells. It is well known that cells infected with a virus are significantly modified and no longer follow the normal biological processes. In this sense, an infected cell is transformed into a new living organism which has its own death process. This new death process yields the average death rate of a population of infected cells. This new death rate is what we have defined as the virulence of the infecting viral strain. In the case of coinfected cells we assume that this is imposed by the less virulent infecting strain (see Box below). Accordingly, the time evolution of the concentration of two competing viral strains, uninfected and infected cells is described by the following system of ordinary differential equations

$$\begin{aligned} \dot{x} &= \lambda - dx - \beta x(v_1 + v_2) \\ \dot{y}_1 &= \beta x v_1 - \beta y_1 v_2 - a_1 y_1 \\ \dot{y}_2 &= \beta x v_2 - \beta y_2 v_1 - a_2 y_2 \\ \dot{y}_{12} &= \beta(y_1 v_2 + y_2 v_1) - \min(a_1, a_2) y_{12} \\ \dot{v}_1 &= K a_1 y_1 + cK \min(a_1, a_2) y_{12} - u v_1 \\ \dot{v}_2 &= K a_2 y_2 + (1-c) K \min(a_1, a_2) y_{12} - u v_2 \end{aligned} \tag{1}$$

The variable x models the concentration of uninfected cells with an external constant supply of new cells at rate λ, dying at a rate d and being infected with efficiency β. The variable v_1 respectively v_2 describes the concentration of strain 1 respectively strain 2. The variable y_i represents the concentration of cells infected solely with strain i. These cells die and release viral offspring at rate a_i, the virulence of strain i. The variable y_{12} models the concentration of cells infected with both viral strains. These cells die and release viral offspring at rate $\min(a_1, a_2)$ (more on this below). Free virus of type i is produced at rate $k_i = Ka_i$, where K is the burst size, and inactivated at rate u. The parameter c denotes the proportion of strain 1 produced at the burst of coinfected cells y_{12}. The state of the system at time t is denoted $S(t) = (x(t),\, y_1(t),\, y_2(t),\, y_{12}(t),\, v_1(t),\, v_2(t))^T$.

We make the following general assumptions about the parameters:

- All parameters are positive.
- The efficiency with which strain 1 respectively strain 2 infects uninfected cells or singly infected cells (y_1 or y_2) is equal and denoted by β.
- The death rates of strain 1 respectively strain 2 are equal and denoted by u.

Furthermore, based on the experimental results presented in Ojosnegros et al. (31), see Box below, we assume:

- The burst size of singly and coinfected cells is equal and denoted by K.
- The death rate of coinfected cells is equal to the death rate of cells singly infected with the least virulent virus, $a_{12} = \min(a_1,\, a_2)$. In other words, this rate is imposed by the least virulent viral strain.

- To account for the competition-colonization trade-off postulated, we model the intracellular fitness of the viruses during coinfection as being inversely proportional to their respective virulence by setting $c := a_1^{-1}/(a_1^{-1} + a_2^{-1})$. In this simple relationship we capture the assumption that poor colonization abilities are compensated by intracellular competition abilities and vice versa.

Without loss of generality, we can assume $a_1 \leq a_2$. Thus, strain 1 is the better competitor and strain 2 is the better colonizer and the last three equations of (1) become

$$\begin{aligned} \dot{y}_{12} &= \beta y_1 v_2 + \beta y_2 v_1 - a_1 y_{12} \\ \dot{v}_1 &= K a_1 y_1 + c K a_1 y_{12} - u v_1 \\ \dot{v}_2 &= K a_2 y_2 + (1-c) K a_1 y_{12} - u v_2 \end{aligned}$$

In Ojosnegros et al. (31), the model (1) with $\lambda = 0$, $d = 0$, $a_1 < a_2$ and an unconstrained (i.e. independent of a_1) parameter $c > 1/2$, was introduced to describe two competing viral strains in cell culture. These special *in vitro* conditions of a fixed and limited amount of target cells allowed for an analytical treatment of the system in the large initial virus load limit which is not possible in the more general case of system (1) considered here.

Ojosnegros et al. (31) described the diversification of a single purified clone of foot-and-mouth disease virus into a two populations that resembled the ecology strategies of competition and colonization.
The phenotype of the two strategies showed the following main features:

- Colonizers are virulent variants with higher cell killing rate
- Competitors kill the cells slower than colonizers, but when competitors and colonizers infect the same cell, the cell die slowly, as when infected only by competitors.
- Competitors and colonizers show identical progeny production, that is, same burst size.
- Competitors however, produce more progeny in coinfected cells. When a cell is coinfected by both variants, the production of each variant is uneven, and competitors are favoured.
- Because of the different replication capacity during independent infections or during coinfections, the competition-colonization strategies follow a density-dependent selection. Under low density of viruses, coinfections are rare, a lot of cells are available and colonizers are faster spreading through them. Under high density of viruses, coinfections are frequent and competitors have an advantage.

3. RESULTS

3.1. Establishing infection

To identify the conditions on the parameters of the model that imply spread of at least one of the viral strains, we analyze the stability of the (obvious) equilibrium point

$$S^{(0)} = (x^{(0)}, y_1^{(0)}, y_2^{(0)}, y_{12}^{(0)}, v_1^{(0)}, v_2^{(0)})^T := (\lambda/d, 0, 0, 0, 0, 0)^T$$

at which the infection dies out. The Jacobian matrix J of system (1) evaluated at $S^{(0)}$ is

$$J(S^{(0)}) = \begin{pmatrix} -d & 0 & 0 & 0 & -\beta\lambda/d & -\beta\lambda/d \\ 0 & -a_1 & 0 & 0 & \beta\lambda/d & 0 \\ 0 & 0 & -a_2 & 0 & 0 & \beta\lambda/d \\ 0 & 0 & 0 & -a_1 & 0 & 0 \\ 0 & Ka_1 & 0 & cKa_1 & -u & 0 \\ 0 & 0 & Ka_2 & (1-c)Ka_1 & 0 & -u \end{pmatrix}$$

The eigenvalues of this matrix are

$$-d, \quad -a_1, \quad \frac{-d(a_i+u)+\Delta_i}{2d}, \quad \frac{-d(a_i+u)-\Delta_i}{2d}, \qquad i = 1, 2,$$

where $\Delta_i := \sqrt{d^2(a_i-u)^2 + 4Ka_i\beta\lambda d}$ for $i = 1, 2$. All eigenvalues are real given that all parameters are assumed to be positive. This equilibrium becomes unstable as soon as at least one eigenvalue is positive. This happens if and only if $-d(a_1+u)+\Delta_1 > 0$ or $-d(a_2+u)+\Delta_2 > 0$ which is equivalent to $d(a_1-u)^2 + 4Ka_1\beta\lambda > d(a_1+u)^2$ or $d(a_2-u)^2 + 4Ka_2\beta\lambda > d(a_2+u)^2$. The latter expression is in turn equivalent to $K\beta\lambda > du$. In other words, it is sufficient for viral spread that

$$R_0 := \frac{K\beta\lambda}{du} > 1 \tag{2}$$

For generic parameter values (the fine tuning $K\beta\lambda = du$ cannot be expected), this condition is also necessary, because $K\beta\lambda < du$ implies that $S^{(0)}$ is asymptotically stable.

If we consider initial conditions in which $y_i(0) = 0$, $y_{12}(0) = 0$, $v_i(0) = 0$ and $v_j(0) \neq 0$, where $i, j \in \{1, 2\}, i \neq j$, the model reduces to a simple SIR model of single viral infection (Bonhoeffer et al. (5), Nowak and May (30), see also Korobeinikov (22) for global results) and we recognize the magnitude R_0 as the well known *basic reproductive number* of the infection system. Condition (2) can also be expressed as $M := K\beta\lambda - du > 0$. The magnitude M turns out to be algebraically very helpful for our further analysis of the model.

Having determined a condition on the parameter values that characterizes the event of viral spread, we next ask whether under these circumstances, the system admits a steady state in which both viral strains can coexist. The opposite steady state scenario would be that one of the viral strains outcompetes the other. To this end, we examine further fixed points of the system and their stability.

3.2. Further fixed points

Performing algebraic manipulations we found the following non-trivial fixed points of the system (1):

$$S^{(1)} = \begin{pmatrix} x^{(1)} \\ y_1^{(1)} \\ y_2^{(1)} \\ y_{12}^{(1)} \\ v_1^{(1)} \\ v_2^{(1)} \end{pmatrix} := \frac{1}{\beta} \begin{pmatrix} u/K \\ M/(a_1 K) \\ 0 \\ 0 \\ M/u \\ 0 \end{pmatrix}$$

$$S^{(2)} = \begin{pmatrix} x^{(2)} \\ y_1^{(2)} \\ y_2^{(2)} \\ y_{12}^{(2)} \\ v_1^{(2)} \\ v_2^{(2)} \end{pmatrix} := \frac{1}{\beta} \begin{pmatrix} u/K \\ 0 \\ M/(a_2 K) \\ 0 \\ 0 \\ M/u \end{pmatrix}$$

and

$$S^* = \begin{pmatrix} x^* \\ y_1^* \\ y_2^* \\ y_{12}^* \\ v_1^* \\ v_2^* \end{pmatrix} := \frac{1}{\beta K} \begin{pmatrix} u \\ a_2 u M/(a_1(M + u(a_1 + a_2))) \\ a_1 u M/(a_2(M + u(a_1 + a_2))) \\ M^2/(a_1(M + u(a_1 + a_2))) \\ a_2 K M/(u(a_1 + a_2)) \\ a_1 K M/(u(a_1 + a_2)) \end{pmatrix}$$

By the assumed positivity of the parameters and by $M > 0$ (we assume that viral spread is possible) all these fixed points are (component-wise) non-negative and thus biologically meaningful. We also found a fourth fixed point S^- which, nevertheless, has negative entries for all parameter values considered. Summarizing, we have two equilibria, $S^{(1)}$ and $S^{(2)}$, in which one of the viral strains outcompetes the other, and one coexistence equilibrium S^*. The following subsections are devoted to studying their properties.

3.3. The coexistence equilibrium

The Jacobian matrix $J(S^*)$ of system (1) evaluated at the equilibrium point S^* equals

$$\begin{pmatrix} -\beta\lambda K/u & 0 & 0 & 0 & -u/K & -u/K \\ \frac{a_2 M}{u(a_1+a_2)} & -\frac{a_1 M}{u(a_1+a_2)} - a_1 & 0 & 0 & u/K & -\frac{a_2 u M}{a_1 K(M+u(a_1+a_2))} \\ \frac{a_1 M}{u(a_1+a_2)} & 0 & -\frac{a_2(M+u(a_1+a_2))}{u(a_1+a_2)} & 0 & -\frac{a_1 u M}{a_2 K(M+u(a_1+a_2))} & u/K \\ 0 & \frac{a_1 M}{u(a_1+a_2)} & \frac{a_2 M}{u(a_1+a_2)} & -a_1 & \frac{a_1 u M}{a_2 K(M+u(a_1+a_2))} & \frac{a_2 u M}{a_1 K(M+u(a_1+a_2))} \\ 0 & K a_1 & 0 & \frac{K a_1 a_2}{(a_1+a_2)} & -u & 0 \\ 0 & 0 & K a_2 & \frac{K a_1^2}{(a_1+a_2)} & 0 & -u \end{pmatrix}$$

The characteristic polynomial of this matrix is too long to be displayed. Thus, we performed its analysis using computer algebra and symbolic computation. Under the premise of viral spread,

i.e. $M > 0$, we used the computer algebra system Maple$^{\mathrm{TM}}$ to show that all coefficients are positive. Furthermore, we used Maple$^{\mathrm{TM}}$ to construct Routh's table (Barnett and Šiljak (2)) and verified that all entries in its first column are positive (see supplementary material). By Routh's criterion (Barnett and Šiljak (2)), all roots of the characteristic polynomial have strictly negative real parts. As a consequence, the equilibrium point S^* in which both viral strains can coexist is a local asymptotically stable fixed point. This holds for all positive parameter values, provided $M > 0$.

The peculiarity of this coexistence equilibrium is that the viral load at equilibrium of the competitor, $v_1^* = a_2 M/(\beta u(a_1 + a_2))$, is proportional to the *relative* virulence of the colonizer. Similarly, the viral load at equilibrium of the colonizer, $v_2^* = a_1 M/(\beta u(a_1 + a_2))$, is proportional to the relative virulence of the competitor. Thus, the two-viral-strains system (1) not only allows for coexistence of both viral strains, but it confers the less virulent competitor a reproductive advantage over the more virulent colonizer. This discrepancy is reflected in the higher concentration of competitors, $v_1^*/v_2^* = a_2/a_1 > 1$, and the higher concentration of cells infected with competitors, $y_1^*/y_2^* = (a_2/a_1)^2 > 1$, at equilibrium.

Here the question arises as to which features of the model are responsible for the peculiar properties of the coexistence equilibrium. The two major assumptions in our model are the competition-colonization trade-off, $c = a_1^{-1}/(a_1^{-1} + a_2^{-1})$, and the cell killing rate imposed by competitors in coinfected cells, i.e. the factor $\min(a_1, a_2)$ in the last three equations of model (1). The second assumption turns out to be not crucial, which can be seen as follows. If we replace the minimum in model (1) by the maximum and assume $a_1 \leq a_2$ as before, then we obtain

$$\begin{aligned}
\dot{y}_{12} &= \beta(y_1 v_2 + y_2 v_1) - a_2 y_{12} \\
\dot{v}_1 &= K a_1 y_1 + c K a_2 y_{12} - u v_1 \\
\dot{v}_2 &= K a_2 y_2 + (1-c) K a_2 y_{12} - u v_2
\end{aligned}$$

for the last three equations, while all others remain unchanged. Comparing this model to the original one we realize that strain 1 and strain 2 have interchanged their roles in the sense that the equation for strain 1 now has mixed virulence terms whereas the one for strain 2 has become homogeneous. In other words, we might as well write the maximum model as

$$\begin{aligned}
\dot{x} &= \lambda - dx - \beta x(v_1 + v_2) \\
\dot{y}_2 &= \beta x v_2 - \beta y_2 v_1 - a_2 y_2 \\
\dot{y}_1 &= \beta x v_1 - \beta y_1 v_2 - a_1 y_1 \\
\dot{y}_{12} &= \beta y_1 v_2 + \beta y_2 v_1 - a_2 y_{12} \\
\dot{v}_2 &= K a_2 y_2 + \widetilde{c} K a_2 y_{12} - u v_2 \\
\dot{v}_1 &= K a_1 y_1 + (1-\widetilde{c}) K a_2 y_{12} - u v_1
\end{aligned}$$

where $\widetilde{c} := a_2^{-1}/(a_1^{-1} + a_2^{-1})$. This model is equivalent to (1) with a_1 and a_2 having switched their roles. The coexistence equilibrium in the maximum model is

$$\begin{pmatrix} x^* \\ y_2^* \\ y_1^* \\ y_{12}^* \\ v_2^* \\ v_1^* \end{pmatrix} = \frac{1}{\beta K} \begin{pmatrix} u \\ a_1 u M/(a_2(M + u(a_2 + a_1))) \\ a_2 u M/(a_1(M + u(a_2 + a_1))) \\ M^2/(a_2(M + u(a_2 + a_1))) \\ a_1 M K/(u(a_2 + a_1)) \\ a_2 M K/(u(a_2 + a_1)) \end{pmatrix}$$

at which competitors are more abundant than colonizers both as free virus, $v_1^*/v_2^* = a_2/a_1 > 1$, and inside cells, $y_1^*/y_2^* = (a_2/a_1)^2 > 1$.

We have compared the effect of the cell killing rate of coinfected cells on the steady state by testing the smallest and the biggest values biologically plausible, namely, $\min(a_1, a_2)$ and $\max(a_1, a_2)$. We argue that any value in between (i.e., $a_{12} \in (\min(a_1, a_2), \max(a_1, a_2))$) would not make a difference. Simulation results not presented here support this. Therefore, the comparison of the minimum and the maximum models lets us conclude:

1. How two different viral strains "compromise" within a coinfected cell regarding the cell killing velocity does not affect the steady state properties of the two-viral-strains model.

2. The crucial property is the inverse proportionality between virulence and intracellular fitness during coinfection.

The functional shape $c = a_1^{-1}/(a_1^{-1} + a_2^{-1})$ of this trade-off certainly plays a fundamental role. It would go beyond the scope of this article to analyze the effect of other functional dependencies between virulence a_i and intracellular fitness c; (see Discussion).

3.4. Single viral strain equilibria

The existence of a local asymptotically stable coexistence equilibrium suggests that a viral strain can bear the presence of another one. However, to fully address the question as to whether system (1) always allows for a second viral strain to invade tissue already infected with a different strain, we examine the stability of the equilibria $S^{(1)}$ and $S^{(2)}$, in which one of the viral strains extrudes the other.

The Jacobian matrix of system (1) evaluated at the point $S^{(1)}$ is

$$J(S^{(1)}) = \begin{pmatrix} -M/u - d & 0 & 0 & 0 & -u/K & -u/K \\ M/u & -a_1 & 0 & 0 & u/K & -M/(a_1 K) \\ 0 & 0 & -\frac{M}{u} - a_2 & 0 & 0 & u/K \\ 0 & 0 & M/u & -a_1 & 0 & M/(a_1 K) \\ 0 & Ka_1 & 0 & Ka_1 a_2/(a_1 + a_2) & -u & 0 \\ 0 & 0 & Ka_2 & Ka_1^2/(a_1 + a_2) & 0 & -u \end{pmatrix}$$

Assuming viral spread, ($M > 0$), we showed that the leading coefficient of the characteristic polynomial of $J(S^{(1)})$ is positive, whereas the independent coefficient is negative (see supplementary material). By Routh's criterion, at least one root of the characteristic polynomial has positive real part. Therefore, the equilibrium point $S^{(1)}$ in which the competitor outcompetes the colonizer is not stable. Analogously, we found that the equilibrium point $S^{(2)}$ in which the colonizer outcompetes the competitor is also unstable. Both statements hold true for all positive parameter values, provided that $M > 0$.

However, it is worth mentioning that any trajectory $S(t)$, for which one viral strain, say of type i, and all cells infected or coinfected with it have disappeared at some point in time s, would stay confined in the corresponding hyperplane $H_i := \{(x, y_1, y_2, y_{12}, v_1, v_2)^T \mid y_i = y_{12} = v_i = 0\}$ for all $t \geq s$. As mentioned in Subsection 2, *within* the corresponding hyperplanes, the equilibria $S^{(1)}$ and $S^{(2)}$ become asymptotically stable, provided $R_0 > 1$. Whether a trajectory starting outside H_i flows into the hyperplane or not remains to be analytically studied. Our simulations do not show any evidence for this type of behavior.

3.5. Multiple-viral-strains model

A straightforward generalization of our model (1) that accounts for the experimentally observed diversity of viral populations is to consider more than two competing viral strains. This generalization raises the question of how many viruses can coinfect a cell simultaneously. For example, the multiplicity of HIV-infected spleen cells has been reported between 1 and 8 with mean 3.2 (Jung et al. (20)). However, for the sake of mathematical simplicity, we consider here the case in which at most two viruses can coinfect a cell. We assume that we can distinguish each of the viral strains via their corresponding virulences a_i. As above, we assume inverse proportionality between virulence and intracellular fitness during coinfection. In other words, the proportion of strain i produced at the burst of cells y_{ij} coinfected with v_i and v_j is given by $c_i := a_i^{-1} / \left(a_i^{-1} + a_j^{-1}\right)$, for all $i, j \in \{1, ..., n\}$, $i < j$, where $n \in \mathbb{N}$ is the total number of viral strains modeled. Thus, the equations for the generalized model read:

$$
\begin{aligned}
\dot{x} &= \lambda - dx - \beta x \sum_{j=1}^{n} v_j \\
\dot{y}_i &= \beta x v_i - \beta y_i \left(\sum_{\substack{j=1 \\ j \neq i}}^{n} v_j \right) - a_i y_i, \quad i = 1, ..., n \\
\dot{y}_{lj} &= \beta(y_l v_j + y_j v_l) - \min(a_l, a_j) y_{lj}, \quad l, j = 1, ..., n \text{ and } l < j \\
\dot{v}_i &= K a_i y_i + a_i^{-1} K \left(\sum_{\substack{l,j \\ l<j}} \frac{1}{a_l^{-1} + a_j^{-1}} w_i(l, j) \min(a_l, a_j) y_{lj} \right) - u v_i, \quad i = 1, ..., n
\end{aligned}
$$

where $w_i(l, j) = 1$ if $l = i$ or $j = i$, and otherwise $w_i(l, j) = 0$. The model does not explicitly account for the order of infection. Nevertheless, to increase the symmetry of the model and to simplify the notation, we will consider the order of infection events and separately model the populations y_{lj} and y_{jl}, where the order of the indices indicates the order of infection with the viral strains v_l and v_j. With this notation, in general, $y_{lj} \neq y_{jl}$, and the variable y_{12} in the two-viral-strains model (1) refers to $y_{12} + y_{21}$. To be consistent, we have to make sure that for $l \neq j$, the magnitude $y_{lj} + y_{jl}$ obeys the corresponding equation, that is

$$\dot{y}_{lj} + \dot{y}_{jl} = \beta(y_l v_j + y_j v_l) - \min(a_l, a_j)(y_{lj} + y_{jl})$$

To ensure this, the equation for y_{lj} becomes

$$\dot{y}_{lj} = \beta y_l v_j - \min(a_l, a_j) y_{lj}, \quad l, j = 1, ..., n \text{ s.t. } l \neq j$$

Summarizing, we obtain the following model

$$\begin{aligned}
\dot{x} &= \lambda - dx - \beta x \sum_{j=1}^{n} v_j \\
\dot{y}_i &= \beta x v_i - \beta y_i \left(\sum_{\substack{j=1 \\ j\neq i}}^{n} v_j \right) - a_i y_i, \quad i = 1, ..., n \\
\dot{y}_{lj} &= \beta y_l v_j - \min(a_l, a_j) y_{lj}, \quad l, j = 1, ..., n \text{ s.t. } l \neq j \qquad (3) \\
\dot{v}_i &= K a_i y_i + a_i^{-1} \left(\sum_{\substack{j=1 \\ j\neq i}}^{n} \frac{1}{a_i^{-1} + a_j^{-1}} K \min(a_i, a_j)(y_{ij} + y_{ji}) \right) - u v_i, \quad i = 1, ..., n
\end{aligned}$$

Note that the magnitude $\sum_{j=1}^{n} v_j(t)$ is the total viral population at any given point in time t.

Since the number of equations in this model grows quadratically with the number n of viral strains, it becomes rather involved to analyze it. In (Ojosnegros et al., in preparation) the results of numerical simulation for numerically tractable values of n are presented. Here, in compliance with the quasispecies view of viral populations, we devise a new approach to studying the evolution of virulence and consider the continuum limit of the multistrain model (3). In this continuum limit, we consider a continuous spectrum of virulence values and identify viral strains with virulence values. We call the resulting continuum limit the continuous-virulence model. In this model the viral quasispecies is represented by a time-dependent continuous distribution of virulence. Unlike the discrete multiple-viral-strains model, the continuum approach allows us to study the virulence distribution of diverse RNA virus populations in a manner independent of the number of different strain types.

3.6. Continuous-virulence model

We identify viral strains with their virulence a and denote by $v(a, t)$ the density of viruses of type a at time t. If we consider an interval $[a_1, a_2] \subset (0, 1)$ of possible virulences (in the next Subsection we describe in more detail what we mean by the interval of possible virulences), then the initial distribution of virulences is defined by a continuous density function $v(\cdot, 0) : \mathbb{R} \to \mathbb{R}$ which vanishes outside the interval $[a_1, a_2]$. The continuum limit of model (3) is therefore the following initial value

problem (also known as Cauchy problem):

$$\begin{aligned}
\dot{x}(t) &= \lambda - dx(t) - \beta x(t) \int_{a_1}^{a_2} v(\xi,t)d\xi \\
\frac{\partial y}{\partial t}(a,t) &= \beta x(t)v(a,t) - \beta y(a,t)\left(\int_{a_1}^{a_2} v(\xi,t)d\xi\right) - ay(a,t) \\
\frac{\partial z}{\partial t}(a,b,t) &= \beta y(a,t)v(b,t) - \min(a,b)z(a,b,t) \qquad (4) \\
\frac{\partial v}{\partial t}(a,t) &= Kay(a,t) + a^{-1}K\left(\int_{a_1}^{a_2} \frac{1}{a^{-1}+b^{-1}}\min(a,b)(z(a,b,t)+z(b,a,t))db\right) - uv(a,t) \\
x(0) &= x_0,\ y(\xi,0) = y_0(\xi),\ z(\vartheta,\mu,0) = z_0(\vartheta,\mu),\ v(\xi,0) = v_0(\xi)
\end{aligned}$$

For every $t \in \mathbb{R}_{\geq 0}$, the function $z(\cdot,\cdot,t) : [a_1,a_2]\times[a_1,a_2] \to \mathbb{R}$ describes the density of coinfected cells with respect to the two-dimensional (Lebesgue) measure on $\mathbb{R}^2$. The value $z(a,b,t)$ is only meaningful for our modeling purposes outside the diagonal $a = b$. Note that the exception $j \neq i$ in the sums of the original discrete model can be neglected here because the values of a real valued function on a set of measure zero do not modify the value of the integral.

In the Appendix A we provide a proof of existence of solutions of the system (4).

3.6.1. Simulation results

In order to explore the dynamics of the continuous-virulence model, we numerically solved the Cauchy problem (4), as described in more detail in Appendix B, using typical parameter values given in Table 1. Because y, z, and v represent concentration densities, the units of y and v are [concentration]/[virulence] and the unit of z is [concentration]/[virulence]^2. Given that the unit of virulence is [Time]$^{-1}$, y, z, and v are measured in units of [Time]/[Volume], [Time]^2/[Volume], and [Time]/[Volume], respectively. The variable x represents a concentration and its unit is therefore [Volume]$^{-1}$.

Parameter	**Description**	**Value**	**Units**
λ	Natural growth rate of uninfected population	10^5	$(ml*h)^{-1}$
d	Natural death rate of uninfected population	0.05	h^{-1}
β	Rate of infection	$5\cdot 10^{-8}$	ml/h
K	Burst size	150	Dimensionless
u	Clearance rate of free virus	0.15	h^{-1}

Table 1: Parameters of the model of evolution of virulence during infection

As stated in Section 2, cells infected with a virus are significantly modified and no longer follow the normal biological processes. They obey a new death process which yields the average death rate of a population of infected cells. This new death rate is what we have defined as the virulence of the infecting viral strain. (In the case of coinfected cells we assume that this is imposed by the less virulent infecting strain, see Box above.)

By definition, a death rate must be positive (a negative death rate would imply something like resurrection), thus, we have a first lower bound for possible values of virulence, namely zero. Moreover, the question arises as to whether the death rate of infected cells (i.e., the virulence of the infecting virus) can become lower than the natural death rate of uninfected cells. In the case of oncogenic viruses, this might be possible under certain circumstances, however, we do not intend to consider this type of scenario in this article. In conclusion, we assume that the virulence is bounded below by d, the natural death rate of uninfected cells.

We set the upper limit of the interval of possible virulence values to $1/2\ h^{-1}$ based on general knowledge about how fast RNA viruses can kill a cell [SAMUEL, DO YOU HAVE A REFERENCE FOR THIS?].

The aforementioned lower and upper bounds of virulence imply that, within the framework of our model, the distribution of virulence in a viral population has to be confined to the interval $[a_1, a_2] := [d, 0.5]$. In other words, the support of a distribution's density function must lie within $[d, 0.5]$.

Starting from non infected tissue, i.e. $x_0 = \lambda/d$, $y_0(\xi) \equiv 0$ and $z_0(\vartheta, \mu) \equiv 0$, we studied three different initial *unnormalized* continuous distributions of virulences given by the densities $v(a, 0) = v_0(a)$, $a \in [d, 0.5]$:

1. A uniform distribution defined by $v_0(a) = \mathbf{1}_{[d,0.5]}(a)$, where $\mathbf{1}_{[d,0.5]}$ is the indicator function of the set $[d, 0.5]$. The total initial concentration is given by $\int_{\mathbb{R}} v_0(a)da = \int_d^{0.5} v_0(a)da = 0.450\ ml^{-1}$.

2. A truncated Gaussian distribution with mean value $\mu = 1/4$ and standard deviation $\sigma = 1/40$ given by $v_0(a) = \mathbf{1}_{[d,0.5]}(a)e^{-800(a-1/4)^2}$. The total initial concentration is given by $\int_{\mathbb{R}} v_0(a)da = \int_d^{0.5} v_0(a)da \approx 0.063\ ml^{-1}$.

3. A truncated mixture of two Gaussian distributions with mean values $\mu_1 = 1/6$, $\mu_2 = 4/10$, equal standard deviations $\sigma_1 = \sigma_2 = 1/150$ and unequal weights $\lambda_1 = 3/10$, $\lambda_2 = 7/10$ given by $v_0(a) = \mathbf{1}_{[d,0.5]} C \left((3/7)e^{-11250(a-1/6)^2} + (7/10)e^{-11250(a-4/10)^2} \right)$, where C is a constant. The total initial concentration is given by $\int_{\mathbb{R}} v_0(a)da = \int_d^{0.5} v_0(a)da \approx 0.024\ ml^{-1}$.

The time evolution of a flat initial virulence density is shown in snapshots in Figure 1. After a very short absorption phase, the density takes an exponential shape in favor of the most virulent part of the interval which is greatly amplified during the first thirteen hours of simulation time. After approximately 14 hours a recession is observed, which by $t = 5.9$ *days* has already decreased the populations' densities by one order of magnitude. After approximately 8 days a qualitative change takes place and the distribution starts loosing its exponential shape to become a non-symmetric unimodal distribution with mode around virulence $= 0.275$ at $t = 9.9$ *days*. This distribution starts traveling to the left, becomes narrower and more symmetric. By $t = 19$ *days* the distribution has moved further to the left and is now almost symmetric. At this point, the dynamics become significantly slower and we start observing an amplification effect. At $t = 29$ *days* the distribution starts changing its shape to become an exponentially shaped distribution, this time in favor of low-virulence competitors. The changes become very slow and, at least numerically, the system seems to be reaching a stationary distribution highly in favor of the smallest virulence values. (In

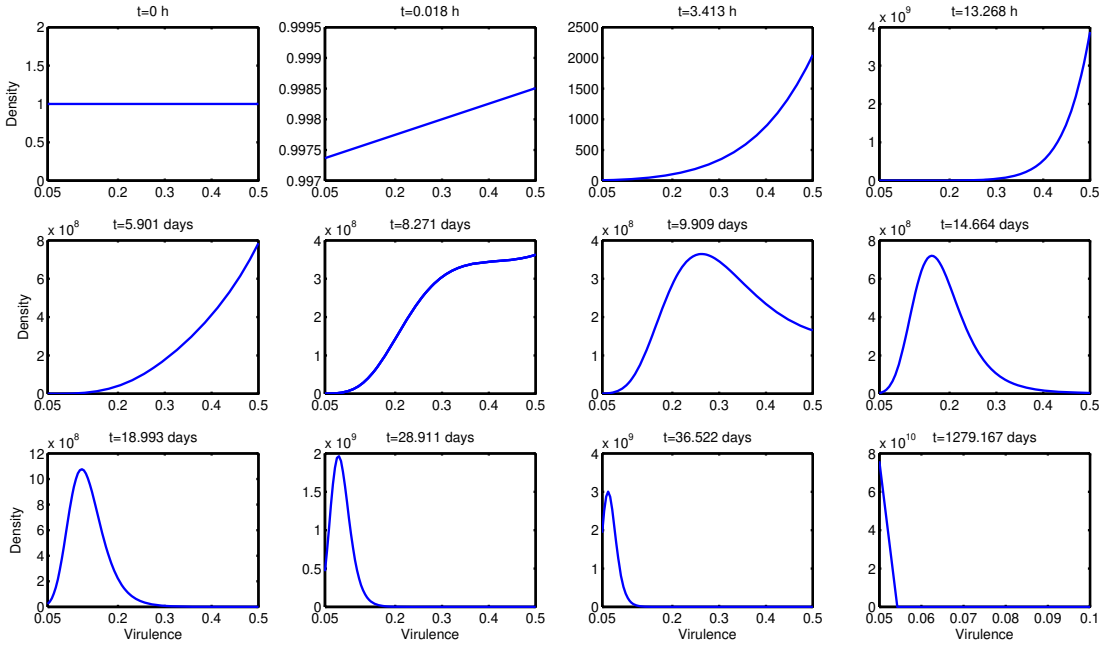

Figure 1. Time evolution of a uniform initial distribution of virulences. Each panel shows the shape of the density function at the point in time displayed in its titel.

the supplementary material we provide movies of the simulations depicted by snapshots in Figures 1,2 and 3.)

Despite the prominent differences between the initial distributions, Figures 2 and 3 reveal similar qualitative properties of the dynamics, namely, a biphasic behavior comprising an initial phase in which the more virulent parts of the density are amplified, followed by a second phase in which the less virulent regions predominate. All three trajectories become very similar once the density becomes unimodal, although the time scales are significantly different, and all three reach very similar numerically stationary distributions (more on this in the next Subsection).

For each of the three initial virulence densities $v_0(a)$, Figure 4 shows the time evolution of the expected value $E(a)$ of the virulence at point in time t, $E(a)(t) = \int_{a_1}^{a_2} \xi v(\xi,t)/\left\|v(b,t)\right\| d\xi$, which is obtained by normalizing with $\|v(b,t)\| := \int_{a_1}^{a_2} v(b,t)db$ at each point in time t, as the system of integro-partial differential equations is not norm-preserving. In this graph, we can clearly identify the two different regimes of the biphasic behavior described above.

This biphasic behavior can also be observed in simulations of the two-viral-strains model (simulations presented in Ojosnegros et al., in preparation). As a matter of fact, the simulations suggest that the coexistence equilibrium (see above) is globally attracting, provided that $M > 0$. If we assume that this equilibrium is globally attracting under the premise of viral spread ($M > 0$), we can immediately follow that starting from initial conditions in which the most virulent virus predominates ($v_2(0) > v_1(0)$), the system must undergo this biphasic behavior. On the other hand, starting from initial conditions in which the least virulent virus predominates ($v_1(0) > v_2(0)$), the differential equations for the viral populations at an early stage in which the number of coinfected

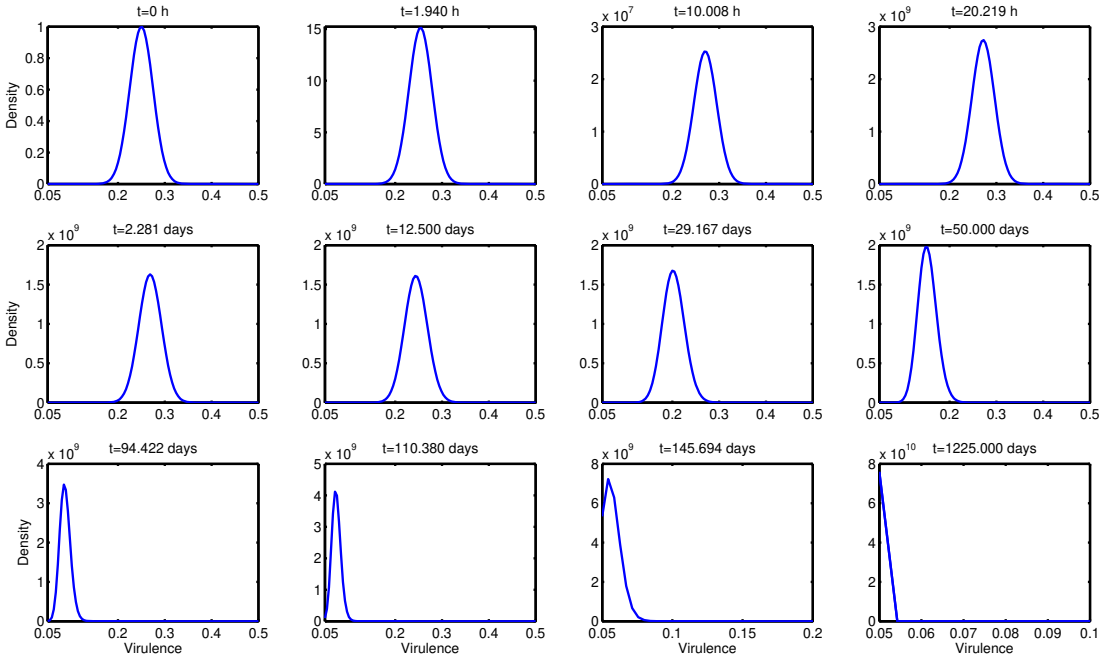

Figure 2: Time evolution of a Gaussian mixture initial distribution of virulences.

cells can be neglected can be written as

$$\begin{aligned} \dot{v}_1 &= K a_1 y_1 - u v_1 \\ \dot{v}_2 &= K a_2 y_2 - u v_2 \end{aligned}$$

From these we can follow that, at an early stage, the population v_2 of the most virulent virus grows faster than the population v_1 of the least virulent one. Depending on the initial values $v_1(0)$ and $v_2(0)$, the most virulent viruses might or might not become more numerous than the least virulent ones during the initial phase.

3.6.2. Analytical assessment of stationary solutions

Given the apparent convergence observed in our three simulation experiments, we speculated whether the exponentially shaped distribution observed towards the end of the simulations would become steeper and steeper and eventually stabilize in the shape of a (Dirac-) delta distribution δ_{a_1} with peak at $a = a_1$. To explore this, we formulated the following Ansatz for the stationary distributions

$$\begin{aligned} y^*(a) &= Y \delta_{a_1}(a) \\ v^*(a) &= V \delta_{a_1}(a) \\ z^*(a,b) &= Z \delta_{(a_1,a_1)}(a,b) \end{aligned} \tag{5}$$

where δ_{a_1} is the one dimensional delta distribution centered at a_1, $\delta_{(a_1,a_1)}$ is the two-dimensional delta distribution centered at (a_1, a_1), and $Y, V, Z \in \mathbb{R}$ are parameters to be determined. For the

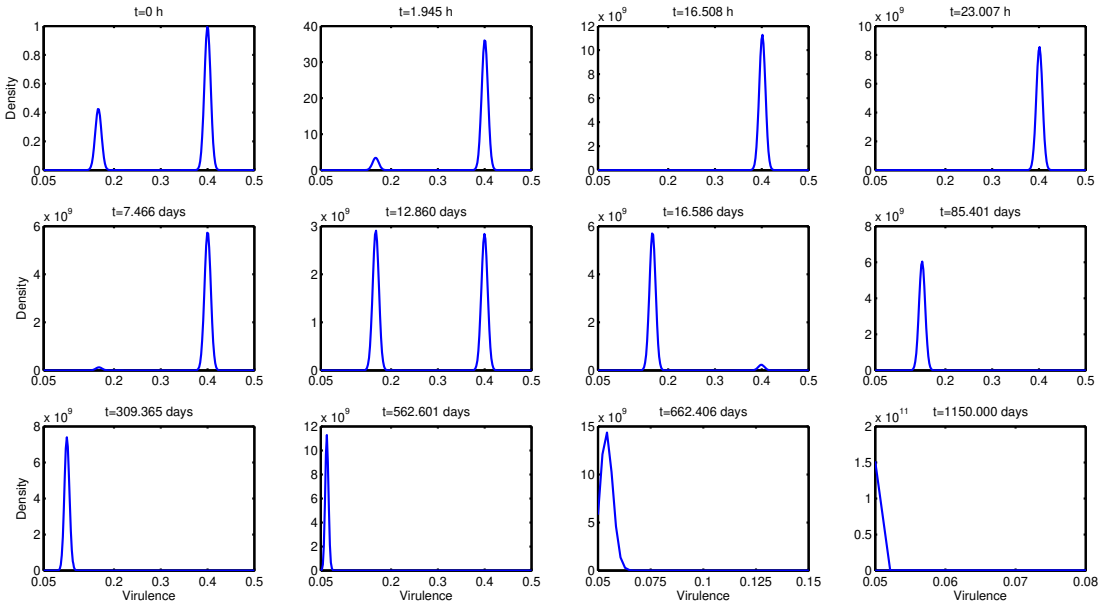

Figure 3: Time evolution of a Gaussian mixture initial distribution of virulences.

x component the stationary value is just a point $x^* \in \mathbb{R}$, a fourth parameter to be determined. In order to obtain conditions that determine these four parameters we assume that the solution postulated is stationary, that is, the right hand side of (4) should vanish in a distributional sense. The first equation of (4) yields (recall $\int_{\mathbb{R}} \delta_{a_1}(\xi)d\xi = \int_{a_1}^{a_2} \delta_{a_1}(\xi)d\xi = 1$)

$$\lambda - dx^* - \beta x^* V = 0 \tag{6}$$

The second and third equation of (4) yield

$$\begin{aligned} \beta x^* V \delta_{a_1}(a) - \beta Y \delta_{a_1}(a) V - aY\delta_{a_1}(a) &= 0 \\ \beta Y \delta_{a_1}(a) V \delta_{a_1}(a) - \min(a,b) Z \delta_{(a_1,a_1)}(a,b) &= 0 \end{aligned}$$

These are to be understood in a distributional sense, that is, for any test function F with support contained in $[a_1, a_2]$ it should hold (recall $\delta_{a_1}(F) = \int_{\mathbb{R}} \delta_{a_1}(\xi)F(\xi)d\xi = F(a_1)$)

$$\begin{aligned} \left(\beta x^* V \delta_{a_1}(a) - \beta Y \delta_{a_1}(a) V - aY\delta_{a_1}(a)\right)(F) &= \int_{\mathbb{R}} \left(\beta x^* V \delta_{a_1}(a) - \beta Y \delta_{a_1}(a) V - aY\delta_{a_1}(a)\right) F(a)da \\ &= \int_{a_1}^{a_2} \left(\beta x^* V \delta_{a_1}(a) - \beta Y \delta_{a_1}(a) V - aY\delta_{a_1}(a)\right) F(a)da \\ &= \beta x^* V F(a_1) - \beta Y V F(a_1) - a_1 Y F(a_1) = 0 \end{aligned}$$

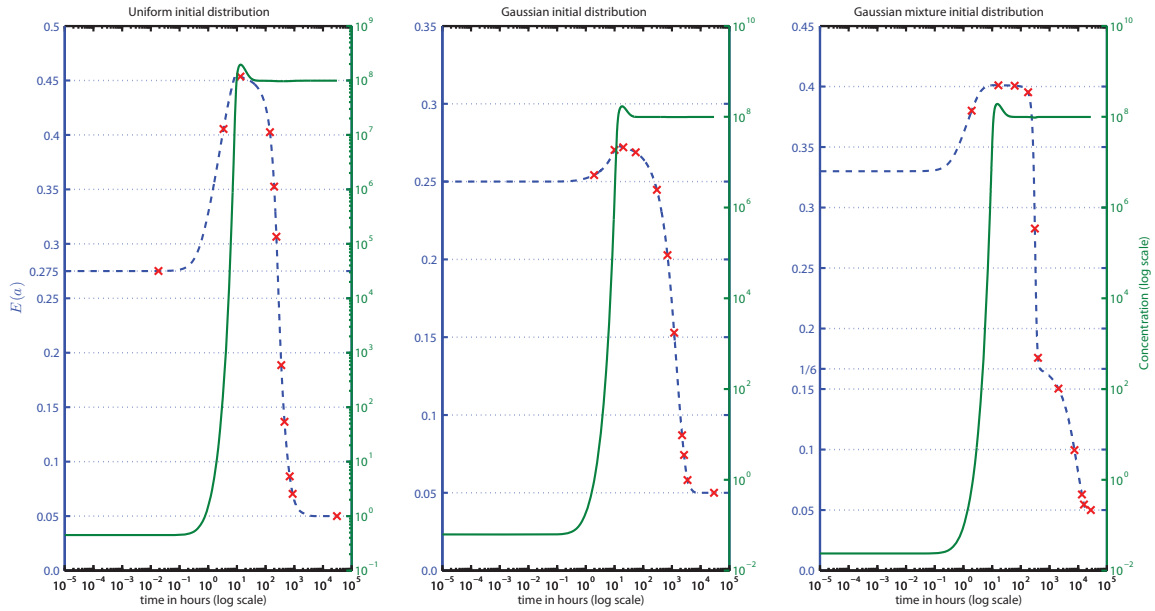

Figure 4. Time evolution of the expected value $E(a)(t) = \int_{a_1}^{a_2} \xi v(\xi,t)/\left\|v(b,t)\right\| d\xi$ of virulence (dashed curve, vertical axes on the left) and of the total concentration of viruses $\int_{a_1}^{a_2} v(b,t)db$ (solid curve, vertical axes on the right) for three different initial distributions. The crosses mark the value of $E(a)$ at the time points (> 0) depicted in the corresponding evolution-of-distribution-figure (Figures 1-3).

Analogously, for any test function F with support contained in $[a_1, a_2] \times [a_1, a_2]$ we require

$$\begin{aligned}
&\left(\beta Y \delta_{a_1}(a) V \delta_{a_1}(b) - \min(a,b) Z \delta_{(a_1,a_1)}(a,b)\right)(F) \\
= &\int_{\mathbb{R}^2} \left(\beta Y \delta_{a_1}(a) V \delta_{a_1}(b) - \min(a,b) Z \delta_{(a_1,a_1)}(a,b)\right) F(a,b) da db \\
= &\int_{a_1}^{a_2} \int_{a_1}^{a_2} \left(\beta Y \delta_{a_1}(a) V \delta_{a_1}(b) - \min(a,b) Z \delta_{(a_1,a_1)}(a,b)\right) F(a,b) da db \\
= &\beta Y V F(a_1,a_1) - a_1 Z F(a_1,a_1) = 0
\end{aligned}$$

In particular, for a function F with $F(a_1) \neq 0$ it holds

$$\beta x^* V - \beta Y V - a_1 Y = 0 \tag{7}$$

And analogously for a function F with $F(a_1, a_1) \neq 0$ we have

$$\beta Y V - a_1 Z = 0 \tag{8}$$

By the same distributional argument, for any test function F with support contained in $[a_1, a_2]$ the fourth equation of (4) yields

$$\begin{aligned}
&\left(KaY\delta_{a_1}(a) + a^{-1}K\left(\int_{a_1}^{a_2} \frac{1}{a^{-1}+b^{-1}} \min(a,b) Z(\delta_{(a_1,a_1)}(a,b) + \delta_{(a_1,a_1)}(b,a))db\right) - uV\delta_{a_1}(a)\right)(F) \\
= &\int_{a_1}^{a_2} KaY\delta_{a_1}(a)F(a)da + K\left(\int_{a_1}^{a_2}\int_{a_1}^{a_2} \frac{a^{-1}}{a^{-1}+b^{-1}} \min(a,b) Z(\delta_{(a_1,a_1)}(a,b) + \delta_{(a_1,a_1)}(b,a))F(a)dbda\right) \\
&- \int_{a_1}^{a_2} uV\delta_{a_1}(a)F(a)da \\
= &\; Ka_1YF(a_1) + Ka_1ZF(a_1) - uVF(a_1) = 0
\end{aligned}$$

Again, for a function F with $F(a_1) \neq 0$ we have

$$Ka_1Y + Ka_1Z - uV = 0 \tag{9}$$

Summarizing, the stationarity argument has provided us with a system of four non-linear equations (6), (7), (8), and (9) for the unknown parameters x^*, Y, Z and V. By solving this system of equations algebraically we obtain

$$L^{(0)} = \begin{pmatrix} x^{(0)} \\ Y^{(0)} \\ Z^{(0)} \\ V^{(0)} \end{pmatrix} := \begin{pmatrix} \lambda/d \\ 0 \\ 0 \\ 0 \end{pmatrix}$$

and

$$L^* = \begin{pmatrix} x^* \\ Y^* \\ Z^* \\ V^* \end{pmatrix} := \frac{1}{\beta K}\begin{pmatrix} u \\ uM/(M+ua_1) \\ M^2/(a_1(M+ua_1)) \\ KM/u \end{pmatrix}$$

where $M = K\beta\lambda - du$ as before.

The solution $L^{(0)}$ represents the state in which the infection dies out. Interestingly, if we simulate the continuous-virulence model using parameters such that the condition for viral spread established for the two-viral-strain model is not fulfilled (i.e., $M < 0$), the system evolves towards this state (results not explicitly shown).

The solution L^* has a remarkable structural similarity with the coexistence solution S^* we found for the two-viral-strain model. However, the corresponding stationary solution cannot be regarded as a coexistence solution, because only the least virulent part of the population survives. The stationarity argument presented above was strongly validated when we confirmed that in each

of the three simulation experiments presented in the previous Subsection the following holds

$$\begin{aligned} x(T) &= x^* \\ \int_{a_1}^{a_2} y(\xi,T)d\xi &= Y^* \\ \int_{a_1}^{a_2}\int_{a_1}^{a_2} z(\xi,\eta,T)d\xi d\eta &\approx Z^* \\ \int_{a_1}^{a_2} v(\xi,T)d\xi &= V^* \end{aligned}$$

where T is the total simulation time run.

This concordance provides strong evidence for the convergence of our simulations towards a stationary solution of (4). There is a small discrepancy in the case of the integral of $z(\xi,\eta,T)$ over $[a_1,a_2]\times[a_1,a_2]$. We attribute this discrepancy to the discretization error that arises during the numerical approximation of the integral using an equidistant grid on $[a_1,a_2]\times[a_1,a_2]$.

With the parameter values L^* obtained, our Ansatz (5) leads us to a non-trivial stationary solution of (4).

4. DISCUSSION

We have analyzed the evolution of virulence of an RNA viral quasispecies in which the cell killing capacity (what we call the virulence a_i) of viruses is inversely related to the intracellular viral fitness within coinfected cells. In the case of two viral strains, this competition-colonization trade-off allows for stable coexistence of competitors and colonizers and each virus type can be invaded by the other, whenever the conditions for viral spread are given. These conditions do not depend on the particular virulence values a_i. However, the population levels at the coexistence equilibrium do depend on the particular virulence values a_i, and, as we saw above, this dependency is in favor of the least virulent viral strain.

Generalizing this two-viral-strains model to multiple viral strains is conceptually straightforward, but the resulting system of differential equations is difficult to study analytically. Moreover, the lack of accurate experimental measurements of the actual number of (in terms of virulence) different strains contained in a phenotypically diverse viral population limits the applicability of this modeling approach. Furthermore, the quadratic dependency of the number of equations on the number of strains n (recall Subsection 3.5) constrains the dimension of the models that can be numerically analyzed (Kryazhimskiy et al. (24)). We circumvented these issues by considering a continuous spectrum of virulence values and postulating a model that would describe the time evolution of a continuous distribution of virulences under the same type of competition-colonization trade-off. This model of continuous virulence is naturally derived as the continuum limit of the multiple-viral-strains model, thus providing a better modeling framework for the very high phenotypic diversity of viral populations. While the model exhibits a complicated mathematical structure as an integro-differential Cauchy problem (Cushing (12)), we were able to provide a simple proof of the existence of solutions. Having clarified the issue of existence of solutions, we solved this

Cauchy problem numerically using typical parameter values. The discretization step size in the numerical scheme (see Appendix B), clearly limits the accuracy of the numerical approximations. However, this numerical limitation does not represent a loss of modeling power, whereas, as explained above, computational issues do limit the number of scenarios that can be modeled with the discrete multiple-strains model.

Our simulation results indicate that the intra-host evolution of virulence is characterized by two phases. During the first phase, colonizers become more frequent and the average virulence of the population increases. In the second phase, the abundance of competitors increases and the mean population virulence decreases. Eventually, the virulence distribution takes an exponential shape in favor of the least virulent part of the population. In our simulations, this distribution seems to be converging towards $V\delta_{a_1}$, where δ_{a_1} is the delta distribution centered at a_1 and $V \in \mathbb{R}$ a suitable constant (see Subsection 3.6.2). However, this convergence process takes infinite time, implying that, after a finite period of time (in our simulations ranging from 1 month to 1.8 years), the exponentially shaped distribution in favor of the least virulent part of the population becomes the qualitatively characteristic state of the intra-host viral population.

To investigate the consistency of our modeling approach, we compared the qualitative properties of the dynamics displayed by the continuous-virulence model (4) and the qualitative properties of the dynamics displayed be the discrete multiple-viral-strains model (3) (simulation results presented in Ojosnegros et al., in preparation). Assuming that viral spread is possible (i.e., $M > 0$), we found that the basic biphasic feature, namely, an initial phase in which the more virulent strains colonize and expand, followed by a second phase in which the less virulent strains predominate, is present in the dynamics of both models. Also the shapes of the continuous distributions in the course of the simulations show similarity to the ones observed in the discrete case, as long as the discrete virulence values considered in the discrete model are uniformly distributed over the interval $[a_1, a_2] \subset (0, 1)$ of possible virulences. These facts are not surprising, given that the system of ODEs solved to numerically approximate the solution of the continuous virulence system is structurally very similar to the equations of the discrete model, the only difference being the weights that appear in the Newton-Cotes formulas used to approximate the integrals $\int_{a_1}^{a_2} v(\xi, t)d\xi$ and $\int_{a_1}^{a_2} \frac{1}{a^{-1}+b^{-1}} \min(a, b)(z(a, b, t) + z(b, a, t))db$ (see Appendix B). Nevertheless, we found it very interesting that if we simulate the continuous-virulence model using parameters such that the condition for viral spread is not fulfilled (i.e., $M < 0$), the system evolves towards the zero density function (results not explicitly shown). This outcome seems to be independent of the initial distributions of virulence used. This result suggests that the condition for viral spread, which we originally derived for the two-viral-strains model, appears to be still correct in the continuum limit.

On the other hand, the dynamics of the two models do show an important difference: Under viral spread conditions (i.e., $M > 0$), the stationary distributions reached in the continuous and the discrete case differ in that the stationary continuous distribution is extremely more positively skewed and only the very least virulent strains are represented. This finding has unexpected implications for the discrete model (3), which will be discussed elsewhere (Ojosnegros et al., in preparation).

It is well known that RNA viruses replicate with high error rates . We can not discard that mutation plays a role in modulating the evolution of virulence, although in this initial study we have considered a more simplified scenario. In a parallel study (Ojosnegros et al., in preparation), we have analyzed a multistrain model and implemented the model with different initial distributions of virulent mutants. The main outcome of the model, namely the imposition of competitors over colonizers after a transient domination of colonizers, seems to be basically independent of the

initial shape of the population distribution of virulence. In this sense, we anticipate that mutations may alter the distribution causing a resetting of the dynamic process. Accordingly, we speculate that the steady state might occur in the form of a dynamic polymorphism of virulent variants, similar to the one described by the quasispecies model. However, the byphasic behavior of the competition-colonization model might still hold after implementation of mutation mechanisms.

In conclusion, the two models studied in this article make two major predictions about the evolution of virulence under a competition-colonization trade-off. First, two viral strains with distinct virulence can coexist, and second, a viral population displaying a range of virulence values will be attenuated and evolve towards a population of many competitors and very few colonizers. Our model predictions differ from most prognoses based on previous epidemiological models of the evolution of virulence, which often conclude that selection maximizes the basic reproductive number of the pathogen. This discrepancy is due to the following:

1. One key feature of our approach is that we introduce specific variables and equations to model the populations of coinfected cells.

2. We do not assume that the viral strain with the highest individual cell killing performance dominates the events during coinfections.

3. We assume a competition-colonization trade-off.

These three assumptions combined have not been considered in previous modeling approaches. Under these premises, selection appears to favor low-virulence competitors, as long as uninfected cells are constantly replenished, but not unlimited. The attenuation property of the continuous-virulence model may also explain experimental observations of suppression of high-fitness viral mutants (colonizers), which might have been displaced by competitors (de la Torre and Holland (34), Novella et al. (27), Turner and Chao (35), Bull et al. (9)).

In Ojosnegros et al. (31) two foot-and-mouth disease viral strains were reported that had been isolated from a population undergoing viral passaging experiments. Measurement of cell killing rates, intracellular fitness, and other parameters suggested a competition-colonization trade-off. These experimental findings motivated the hypothesis that viruses can specialize either to improve colonization by fast cell killing, or to improve competitive intracellular reproductive success. In our modeling approach, we have implemented the competition-colonization trade-off using the algebraically simple relationship $c = a_1^{-1}/(a_1^{-1} + a_2^{-1})$ which renders the mathematical analysis convenient. The actual dependency between virulence a_i and intracellular fitness c is likely to be more complicated and to depend on additional parameters. It would be of biological interest to identify and to characterize virus populations with a competition-colonization trade-off and to establish the nature of the trade-off experimentally. In this article, our principal aim was to provide a rigorous mathematical analysis of a viral competition model incorporating a simple but archetypical instance of a competition-colonization trade-off.

APPENDIX A. EXISTENCE OF SOLUTIONS OF THE CONTINUOUS-VIRULENCE MODEL'S EQUATIONS

If we assume that a solution of the initial value problem (4) exists, then we can derive the following expressions: Setting $V(t) := \int_{a_1}^{a_2} v(\xi,t)d\xi$ we have, for the first equation, $\dot{x}(t) = \lambda - dx - \beta x(t)V(t)$ and thus

$$x(t) = \left(x_0 + \int_0^t \lambda e^{W(\xi)} d\xi \right) e^{-W(t)} \tag{10}$$

where $W(\theta) := \int_0^\theta d + \beta V(\tau)d\tau$. The second equation can be solved as

$$y(a,t) = \left(y_0(a) + \beta \int_0^t x(\tau)v(a,\tau)e^{U_a(\tau)} d\tau \right) e^{-U_a(t)}$$

where $U_a(\theta) := \int_0^\theta a + \beta V(\tau)d\tau$. Substituting the expression for $x(t)$ into the expression for $y(a,t)$ gives

$$\begin{aligned} y(a,t) &= \left(y_0(a) + \beta \int_0^t v(a,\tau) \left(x_0 + \int_0^\tau \lambda e^{W(\xi)} d\xi \right) e^{U_a(\tau) - W(\tau)} d\tau \right) e^{-U_a(t)} \\ &= \left(y_0(a) + \beta \int_0^t v(a,\tau) \left(x_0 + \int_0^\tau \lambda e^{W(\xi)} d\xi \right) e^{(a-d)\tau} d\tau \right) e^{-U_a(t)} \end{aligned} \tag{11}$$

The third equation yields

$$z(a,b,t) = \left(z_0(a,b) + \beta \int_0^t y(a,\eta)v(b,\eta)e^{\min(a,b)\eta} d\eta \right) e^{-\min(a,b)t} \tag{12}$$

Substituting the expression for $y(a,t)$ allows us to express $z(a,b,t) + z(b,a,t)$ in terms of $v(a,\tau)$, $v(b,\tau)$, and integrals involving them as

$$z(a,b,t) + z(b,a,t) = \left(z_0(a,b) + z_0(b,a) + R(a,b,t) \right) e^{-\min(a,b)t}$$

where

$$\begin{aligned} R(a,b,t) &:= \beta \int_0^t \left(\left(v(b,\eta)y_0(a) + v(a,\eta)y_0(b) + Q(a,b,\eta) \right) e^{\min(a,b)\eta - U_a(\eta)} \right) d\eta \\ Q(a,b,\eta) &:= \beta \int_0^\eta \left(v(b,\eta)v(a,\tau)e^{(a-d)\tau} + v(a,\eta)v(b,\tau)e^{(b-d)\tau} \right) \left(x_0 + \int_0^\tau \lambda e^{W(\xi)} d\xi \right) d\tau \end{aligned}$$

Finally, we substitute the expressions obtained for $y(a,t)$ and $z(a,b,t)$ into the differential

equation for $v(a,t)$ obtaining

$$\frac{\partial v}{\partial t}(a,t) = Ka\left(\left(y_0(a)+\int_0^t \beta v(a,\tau)\left(x_0+\int_0^\tau \lambda e^{W(\xi)}d\xi\right)e^{(a-d)\tau}d\tau\right)e^{-U_a(t)}\right)+$$
$$+a^{-1}K\left(\int_{a_1}^{a_2}\frac{1}{a^{-1}+b^{-1}}\min(a,b)(z_0(a,b)+z_0(b,a)+R(a,b,t))e^{-\min(a,b)t}db\right)-uv(a,t) \quad (13)$$

A solution of the system (4) necessarily has to fulfill this integro-partial differential equation for the function $v(a,t)$. On the other hand, a solution of the latter equation that is continuous on $[a_1,a_2]\times\mathbb{R}$ and partially differentiable with respect to t, and satisfies $v(\xi,0)=v_0(\xi)$, allows for constructing a solution of the system (4) by means of substitution of $v(a,t)$ into the expressions (10), (11), and (12).

In order to show that a solution of (4) exists, we consider solutions during a very short time span $[t_1,t_2]\subset[0,\infty)$ within which the values of $V(t)$ and $z(a,b,t)$ do not significantly change, i.e. $V(t)\approx V_{t_1}:=V(t_1)$ and $z(a,b,t)\approx z_{t_1}(a,b):=z(a,b,t_1)\;\forall\, t\in[t_1,t_2]$. Given that (4) is autonomous, we may as well consider the time interval $[t_1=0,t_2]$. Thus, $W(\theta)\approx\int_0^\theta d+\beta V_0 d\tau=\theta(d+\beta V_0)$, $U_a(\theta)\approx\int_0^\theta a+\beta V_0 d\tau=\theta(a+\beta V_0)\;\forall\;\theta\in[0,t_2]$ and $\int_{a_1}^{a_2}\frac{1}{a^{-1}+b^{-1}}\min(a,b)(z(a,b,t)+z(b,a,t))db$ $\approx\int_{a_1}^{a_2}\frac{1}{a^{-1}+b^{-1}}\min(a,b)(z_0(a,b)+z_0(b,a))db=:S_0(a)\;\forall\;t\in[0,t_2]$. With this, equation (13) becomes

$$\begin{aligned}\frac{\partial v}{\partial t}(a,t) &= Ka\left(y_0(a)+\left(\int_0^t\beta v(a,\tau)\left(x_0+\lambda\frac{e^{\tau(d+\beta V_0)}-1}{d+\beta V_0}\right)e^{(a-d)\tau}d\tau\right)e^{-t(a+\beta V_0)}\right)\\ &\quad +a^{-1}KS_0(a)-uv(a,t)\end{aligned}$$

where $y_0(a)=y(a,0)$, $x_0=x(0)$. Some algebra yields

$$\begin{aligned}\frac{\partial v}{\partial t}(a,t) &= Ka\left(y_0(a)+\left(\beta\lambda\int_0^t\frac{\beta V_0}{d^2+d\beta V_0}v(a,\tau)e^{(a-d)\tau}+\frac{1}{d+\beta V_0}v(a,\tau)e^{\tau(a+\beta V_0)}d\tau\right)e^{-t(a+\beta V_0)}\right)\\ &\quad +a^{-1}KS_0(a)-uv(a,t)\\ &= -uv(a,t)+K\beta\lambda a e^{-t(a+\beta V_0)}\int_0^t\left(\frac{\beta V_0}{d^2+d\beta V_0}e^{(a-d)\tau}+\frac{1}{d+\beta V_0}e^{\tau(a+\beta V_0)}\right)v(a,\tau)d\tau\\ &\quad +Kay_0(a)+a^{-1}KS_0(a)\end{aligned}$$

If we write $e^{-t(a+\beta V_0)}$ as $1+(-a-\beta V_0)t+O(t^2)$ and neglect terms of quadratic order we obtain for t sufficiently small

$$\begin{aligned}\frac{\partial v}{\partial t}(a,t) &= -uv(a,t)+K\beta\lambda a(1+(-a-\beta V_0)t)\int_0^t\left(\frac{\beta V_0}{d^2+d\beta V_0}e^{(a-d)\tau}+\frac{1}{d+\beta V_0}e^{\tau(a+\beta V_0)}\right)v(a,\tau)d\tau\\ &\quad +Kay_0(a)+a^{-1}KS_0(a)\end{aligned}$$

Let us assume for a moment that a three times differentiable solution exists. Differentiation on both sides yields

$$\begin{aligned}\frac{\partial^2 v}{\partial t^2}(a,t) &= -u\frac{\partial v}{\partial t}(a,t) - K\beta\lambda a(a+\beta V_0)\int_0^t \left(\frac{\beta V_0}{d^2+d\beta V_0}e^{(a-d)\tau} + \frac{1}{d+\beta V_0}e^{\tau(a+\beta V_0)}\right) v(a,\tau)d\tau \\ &\quad + K\beta\lambda a(1+(-a-\beta V_0)t)\left(\frac{\beta V_0}{d^2+d\beta V_0}e^{(a-d)t} + \frac{1}{d+\beta V_0}e^{t(a+\beta V_0)}\right) v(a,t)\end{aligned}$$

Again, differentiation on both sides gives

$$\begin{aligned}\frac{\partial^3 v}{\partial t^3}(a,t) &= -u\frac{\partial^2 v}{\partial t^2}(a,t) - K\beta\lambda a(a+\beta V_0)\left(\frac{\beta V_0}{d^2+d\beta V_0}e^{(a-d)t} + \frac{1}{d+\beta V_0}e^{t(a+\beta V_0)}\right) v(a,t) \\ &\quad + K\beta\lambda a(1+(-a-\beta V_0)t)\left(\frac{\beta V_0}{d^2+d\beta V_0}e^{(a-d)t} + \frac{1}{d+\beta V_0}e^{t(a+\beta V_0)}\right)\frac{\partial v}{\partial t}(a,t) \\ &\quad - K\beta\lambda a(a+\beta V_0)\left(\frac{\beta V_0}{d^2+d\beta V_0}e^{(a-d)t} + \frac{1}{d+\beta V_0}e^{t(a+\beta V_0)}\right) v(a,t) \\ &\quad + K\beta\lambda a(1+(-a-\beta V_0)t)\left(\frac{(a-d)\beta V_0}{d^2+d\beta V_0}e^{(a-d)t} + \frac{a+\beta V_0}{d+\beta V_0}e^{t(a+\beta V_0)}\right) v(a,t)\end{aligned}$$

Summarizing we have

$$\begin{aligned}&\frac{\partial^3 v}{\partial t^3}(a,t) + u\frac{\partial^2 v}{\partial t^2}(a,t) - K\beta\lambda a(1+(-a-\beta V_0)t)\left(\frac{\beta V_0}{d^2+d\beta V_0}e^{(a-d)t} + \frac{1}{d+\beta V_0}e^{t(a+\beta V_0)}\right)\frac{\partial v}{\partial t}(a,t) \\ = \; & -2K\beta\lambda a(a+\beta V_0)\left(\frac{\beta V_0}{d^2+d\beta V_0}e^{(a-d)t} + \frac{1}{d+\beta V_0}e^{t(a+\beta V_0)}\right) v(a,t) \\ & + K\beta\lambda a(1+(-a-\beta V_0)t)\left(\frac{(a-d)\beta V_0}{d^2+d\beta V_0}e^{(a-d)t} + \frac{a+\beta V_0}{d+\beta V_0}e^{t(a+\beta V_0)}\right) v(a,t) \qquad (14)\end{aligned}$$

For each $a \in [a_1, a_2]$ the latter equation is a third order ordinary differential equation with variable coefficients. Using standard Lipschitz-continuity arguments (see, for instance, Section 4.3 in Königsberger (21)) it can be shown that for each $a \in [a_1, a_2]$ the initial value problem (14) together with $v(a,0) = v_0(a)$, $\frac{\partial v}{\partial t}(a,0) = -uv_0(a) + Kay_0(a) + a^{-1}KS_0(a)$ and $\frac{\partial^2 v}{\partial t^2}(a,0) = -u\left(-uv_0(a) + Kay_0(a) + a^{-1}KS_0(a)\right) + K\beta\lambda a\left(\frac{\beta V_0}{d^2+d\beta V_0} + \frac{1}{d+\beta V_0}\right)v_0(a)$ (which we assume to be continuous functions of a) must have a unique solution defined on some interval $[0, T_1] \subset [0, \infty)$ of positive length $T_1 \in \mathbb{R}_+$. Given that the coefficients of (14) are continuous functions of a (which can be interpreted as a parameter in the ODE (14) in the framework of a sensitivity analysis) all the solutions $v(a,t)$ must be continuous on $[a_1, a_2] \times [0, T_1]$ (see, for instance, Theorem 6.1 in Epperson (16) and also Subsection 3.1.1 in Deuflhard and Bornemann (13)). This family of solutions allows us to construct a local solution (defined on $[a_1, a_2] \times [0, T_1]$) of (4) by means of substitution of $v(a,t)$ into the expressions (10), (11) and (12). The procedure can be now repeated for a short time interval starting at T_1 yielding the next local solution. A global solution can be obtained by patching together the local solutions and letting the $T_i \to 0$.

APPENDIX B. NUMERICAL SOLUTION OF THE CONTINUOUS-VIRULENCE MODEL'S EQUATIONS

To solve the system of equations (4) numerically, we discretized the "virulence-space" with an equidistant grid $G_n([0.01, 0.5])$ and approximated the integrals $\int_{a_1}^{a_2} v(\xi,t)d\xi \approx \sum_{j \in G_n([0.01,0.5])} \gamma_j v(j,t)$

and $\int_{a_1}^{a_2} \frac{1}{a^{-1}+b^{-1}} \min(a,b)(z(a,b,t)+z(b,a,t))db \approx \sum_{j\in G_n([0.01,0.5])} \gamma_j \frac{1}{a^{-1}+j^{-1}} \min(a,j)(z(a,j,t)+z(j,a,t))$ using a Newton-Cotes quadrature formula of seventh order (with weights γ_j). After this discretization step, we obtain for each pair $(a,b) \in (G_n([0.01,0.5]) \times G_n([0.01,0.5]))$ the following system of ordinary differential equations

$$\begin{aligned}
\dot{x}(t) &= \lambda - dx(t) - \beta x(t) \sum_{j\in G_n([0.01,0.5])} \gamma_j v(j,t) \\
\frac{dy}{dt}(a,t) &= \beta x(t) v(a,t) - \beta y(a,t) \sum_{j\in G_n([0.01,0.5])} \gamma_j v(j,t) - a y(a,t) \\
\frac{dz}{dt}(a,b,t) &= \beta y(a,t) v(b,t) - \min(a,b) z(a,b,t) \\
\frac{dv}{dt}(a,t) &= Kay(a,t) + a^{-1}K \left(\sum_{j\in G_n([0.01,0.5])} \gamma_j \frac{1}{a^{-1}+j^{-1}} \min(a,j)(z(a,j,t)+z(j,a,t)) \right) - uv(a,t)
\end{aligned}$$

The resulting system of coupled ordinary differential equations is solved numerically.

References

[1] Anderson, R.M., May, R.M.: Coevolution of hosts and parasites. Parasitology **85 (Pt 2)**, 411–426 (1982)

[2] Barnett, S., Šiljak, D.D.: Routh's algorithm: a centennial survey. SIAM Rev. **19**(3), 472–489 (1977)

[3] Boldin, B., Diekmann, O.: Superinfections can induce evolutionarily stable coexistence of pathogens. J Math Biol **56**(5), 635–672 (2008). DOI 10.1007/s00285-007-0135-1. URL http://dx.doi.org/10.1007/s00285-007-0135-1

[4] Bonhoeffer, S., Lenski, R.E., Ebert, D.: The curse of the pharaoh: the evolution of virulence in pathogens with long living propagules. Proc Biol Sci **263**(1371), 715–721 (1996). DOI 10.1098/rspb.1996.0107. URL http://dx.doi.org/10.1098/rspb.1996.0107

[5] Bonhoeffer, S., May, R.M., Shaw, G.M., Nowak, M.A.: Virus dynamics and drug therapy. Proceedings of the National Academy of Sciences of the United States of America **94**(13), 6971–6976 (1997). URL http://www.pnas.org/content/94/13/6971.abstract

[6] Bonhoeffer, S., Nowak, M.A.: Mutation and the evolution of virulence. Proc Biol Sci **258**(1352), 133–140 (1994)

[7] Bremermann, H.J., Thieme, H.R.: A competitive exclusion principle for pathogen virulence. J Math Biol **27**(2), 179–190 (1989)

[8] Bull, J.J.: Virulence. Evolution **48**(5), 1423–1437 (1994)

[9] Bull, J.J., Millstein, J., Orcutt, J., Wichman, H.A.: Evolutionary feedback mediated through population density, illustrated with viruses in chemostats. Am Nat **167**(2), E39–E51 (2006). DOI 10.1086/499374. URL http://dx.doi.org/10.1086/499374

[10] Coombs, D., Gilchrist, M.A., Ball, C.L.: Evaluating the importance of within- and between-host selection pressures on the evolution of chronic pathogens. Theor Popul Biol **72**(4), 576–591 (2007). DOI 10.1016/j.tpb.2007.08.005. URL http://dx.doi.org/10.1016/j.tpb.2007.08.005

[11] Cooper, V.S., Reiskind, M.H., Miller, J.A., Shelton, K.A., Walther, B.A., Elkinton, J.S., Ewald, P.W.: Timing of transmission and the evolution of virulence of an insect virus. Proc Biol Sci **269**(1496), 1161–1165 (2002). DOI 10.1098/rspb.2002.1976. URL http://dx.doi.org/10.1098/rspb.2002.1976

[12] Cushing, J.M.: Integrodifferential equations and delay models in population dynamics. Lecture notes in Biomathematics. Springer-Verlag, New York (1977)

[13] Deuflhard, P., Bornemann, F.: Numerische Mathematik 2. de Gruyter Lehrbuch. [de Gruyter Textbook], revised edn. Walter de Gruyter & Co., Berlin (2008). Gewöhnliche Differentialgleichungen. [Ordinary differential equations]

[14] Domingo, E., Holland, J.J.: RNA virus mutations and fitness for survival. Annu Rev Microbiol **51**, 151–178 (1997). DOI 10.1146/annurev.micro.51.1.151. URL http://dx.doi.org/10.1146/annurev.micro.51.1.151

[15] Eigen, M., McCaskill, J., Schuster, P.: Molecular quasi-species. J Phys Chem **92**(24), 6881–6891 (1988)

[16] Epperson, J.F.: An introduction to numerical methods and analysis. Revised edn. Wiley-Interscience [John Wiley & Sons], Hoboken, NJ (2007)

[17] Ewald, P.W.: Host-parasite relations, vectors, and the evolution of disease severity. Ann Rev Ecol Syst **14**, 465–485 (1983)

[18] Frank, S.A.: Models of parasite virulence. Q Rev Biol **71**(1), 37–78 (1996)

[19] Holland, J.J., Torre, J.C.D.L., Steinhauer, D.A.: RNA virus populations as quasispecies. Curr Top Microbiol Immunol **176**, 1–20 (1992)

[20] Jung, A., Maier, R., Vartanian, J., Bocharov, G., Jung, V., Fischer, U., Meese, E., Wain-Hobson, S., Meyerhans, A.: Recombination: Multiply infected spleen cells in hiv patients. Nature **418**, 144–+ (2002)

[21] Königsberger, K.: Analysis 2. 5th edn. Springer, Berlin, Heidelberg (2004)

[22] Korobeinikov, A.: Global properties of basic virus dynamics models. Bull. Math. Biol. **66**(4), 879–883 (2004)

[23] Krakauer, D.C., Komarova, N.L.: Levels of selection in positive-strand virus dynamics. J Evol Biol **16**(1), 64–73 (2003)

[24] Kryazhimskiy, S., Dieckmann, U., Levin, S.A., Dushoff, J.: On state-space reduction in multi-strain pathogen models, with an application to antigenic drift in influenza a. PLoS Comput Biol **3**(8), e159 (2007). DOI 10.1371/journal.pcbi.0030159

[25] Lenski, R.E., May, R.M.: The evolution of virulence in parasites and pathogens: reconciliation between two competing hypotheses. J Theor Biol **169**(3), 253–265 (1994)

[26] May, R.M., Nowak, M.A.: Superinfection, metapopulation dynamics, and the evolution of diversity. J Theor Biol **170**(1), 95–114 (1994). DOI 10.1006/jtbi.1994.1171. URL http://dx.doi.org/10.1006/jtbi.1994.1171

[27] Novella, I.S., Reissig, D.D., Wilke, C.O.: Density-dependent selection in vesicular stomatitis virus. J Virol **78**(11), 5799–5804 (2004). DOI 10.1128/JVI.78.11.5799-5804.2004. URL http://dx.doi.org/10.1128/JVI.78.11.5799-5804.2004

[28] Nowak, M., May, R.: Virus dynamics. Oxford University Press (2000)

[29] Nowak, M.A., May, R.M.: Superinfection and the evolution of parasite virulence. Proc Biol Sci **255**(1342), 81–89 (1994). DOI 10.1098/rspb.1994.0012. URL http://dx.doi.org/10.1098/rspb.1994.0012

[30] Nowak, M.A., May, R.M.: Virus dynamics. Oxford University Press, Oxford (2000). Mathematical principles of immunology and virology

[31] Ojosnegros, S., Beerenwinkel, N., Antal, T., Nowak, M.A., Escarmsa, C., Domingo, E.: Competition-colonization dynamics in an RNA virus. Proc Natl Acad Sci U S A p. in press (2010)

[32] Perelson, A., Nelson, P.: Mathematical analysis of HIV-1 dynamics in vivo. SIAM Review **41**(1), 3–44 (1999)

[33] Tilman, D.: Competition and biodiversity in spatially structure habitats. Ecology **75**, 2–16 (1994)

[34] de la Torre, J.C., Holland, J.J.: RNA virus quasispecies populations can suppress vastly superior mutant progeny. J Virol **64**(12), 6278–6281 (1990)

[35] Turner, P.E., Chao, L.: Prisoner's dilemma in an RNA virus. Nature **398**(6726), 441–443 (1999). DOI 10.1038/18913. URL http://dx.doi.org/10.1038/18913